Air-side Thermal Performance of Crossflow over Alternating Cross-section Flattened Tube Bundle

Amawasee Rukruang[1], Nares Chimres[2], and Jatuporn Kaew-On[2,*]

[1]Energy Engineering Program, Faculty of Engineering, Thaksin University, Phatthalung 93210, Thailand
[2]Mechanical Engineering Program, Faculty of Engineering, Thaksin University, Phatthalung 93210, Thailand
[*]Corresponding author, E-mail: kaew_on@yahoo.com

Abstract

The alternating cross-section flattened (ACF) tube is employed to comprise the test tube bundle in this study. This test tube is placed in a crossflow to evaluate the air-side thermal-hydraulic performance. Two test tube bundles are inline tube arrangements with two tube rows. One is made from the circular tube with a diameter of 6.35 mm, and another is made from the ACF tube with a hydraulic diameter of 4.75 mm. The test sections are made from copper tubes. The test conditions were the water mass flow rate of 0.13 kg/s, the inlet water temperature of 50-60 °C, the dry air inlet bulb temperature of 30-40 °C, and the frontal velocity of 1-5 m/s. The experimental results revealed that the tube geometry significantly affects thermal-hydraulic performance. The experiment will compare the circular tube bundle and the ACF tube bundle on heat transfer and pressure drop characteristics. It is observed that the heat transfer rate and heat transfer coefficient of the ACF tube bundle are higher than those of the circular tube bundle. On the other hand, the pressure drop of the circular tube bundle is higher than that of the ACF tube bundle. The result of the experiment concluded that the ACF tube bundle is a better performance than the circular tube bundle by about 1.08-1.17 times and 1.13-1.46 times by the heat transfer coefficient ratio and goodness factor ratio, respectively.

Keywords**:** *air-side performance, alternating cross-section tube, crossflow heat exchanger, inline tube arrangement, tube bank*

1. Introduction

The heat exchange device has been widely used in the heat exchange processes. A crossflow heat exchanger is one of the famous types employed in the industrial sectors. Heat transfer occurs in a perpendicular direction of two fluids. The crossflow heat exchanger can be divided into three groups (Mangrulkar et al., 2019), namely geometry orientation, finned tube, and combined finned tube and vortex generators. Here, we focused on the geometry orientation in a crossflow heat exchanger. The basic work carried out by Roshko et al. (1955) related to a circular tube bundle placed in a crossflow. They reported that the vortices and wake formations from the tube could be augmented heat transfer. Besides, the non-circular tube bundles were experimentally and numerically investigated on thermal-hydraulic performance in the past decade. The most productive research can be concluded as follows.

Lavasani et al. (2014) examined heat transfer and flow characteristics of the cam-shaped tube bundles. They found that the thermal-hydraulic performance of the cam-shape tube bundle was higher than that of the circular tube bundle about six times within the same equivalent diameter. Mangrulkar et al. (2017) evaluated the thermal-hydraulic performance of a cam-shaped tube bundle using the simulation method. They reported that the friction factor of a cam-shape tube bundle presented a lower value than that of the circular tube bundle. Nu/f ratio and goodness factor of the cam-shaped tube bundle was greater than that of the circular tube about 5 and 9 times, respectively. Ahmed et al. (2015) reported that the pressure loss coefficient of the wing-shape tube bundle increased with increasing an attack angle from 0° to 45°. On the contrary, the pressure loss coefficient decreased with increasing an attack angle from 135° to 180°. Chatterjee and Mondal (2013) revealed that the heat transfer and overall flow of the tandem square tube bundle were sharply enhanced due to a fast mixing behind the obstacle. Li et al. (2018) indicated that the twisted oval tube bundle showed better performance than that of the circular tube bundle having the same

tube arrangement by approximately 25.5-33.3%. Alawadhi (2010) investigated the thermal performance of an inline elliptical tube bundle with a variation of tube inclination by the finite element method. The results revealed that the heat transfer rate and pressure drop increased with increasing inclination of the tube, about 238.59% and 700%, respectively. Another work related to a single non-circular tube placed in a crossflow was proposed by Chen (2007). This research work used a mathematical model to study the flow over an alternating elliptical axis (AEA) tube in a cross-stream. The results showed that the fluid behind the tube had a low convective heat transfer owing to the fluid being unable to absorb heat from the tube in this region.

The thermal-hydraulic performance of the non-circular tube bundles placed in a crossflow has been widely investigated in the open literature. Only one simulation work on the alternating cross-section tube has been published by Chen (2007). He used water as a working fluid for both sides. Thus, as aforementioned details, there is room for more research study by using an alternating cross-section tube placed in a crossflow such as a geometry orientation, working fluid, tube size, and investigated method. Also, the alternating cross-section tube bundle placed in the crossflow does not appear in the open literature (Rukruang et al. 2022). Therefore, this work focused on the experimental investigation of an alternating cross-section flattened (ACF) tube bundle placed in a cross-stream. Heat transfer and pressure drop characteristics of the tube bundles were examined. Finally, the experiment compares the performance of the test tube bundles.

2. Objectives

1) To examine the air-side thermal performance of crossflow over an inline ACF Tube bundle.
2) To compare the thermal-hydraulic performance between the ACF tube bundle and circular tube bundle.

3. Materials and Methods

3.1 ACF tube characteristics

An alternating cross-section flattened (ACF) tube is developed from a flattened tube based on the field synergy principle (Guo et al., 1998). The flattened tube is reshaped to the ACF tube by rotating its cross-sectional. In this study, the ACF tube is defined that each connecting flattened cross-section having a rotating angle (θ) of 90°, as illustrated in Figure 1.

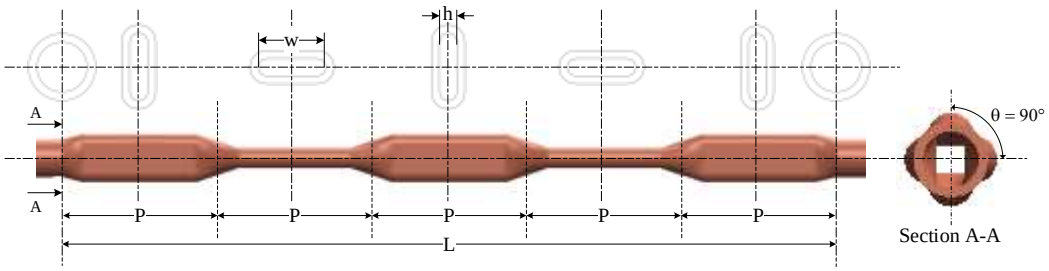

Figure 1 The geometry of the ACF tube

3.2 Experimental apparatus

The schematic diagram of the tube bundles investigation is presented in Figure 2. This diagram consisted of four main parts: air tunnel circuit, hot water circuit, test section, and data acquisition system. The functions of each part are indicated as follows.

(i) Air tunnel circuit: the circuit was used to evaluate the thermal-hydraulic performance of the circular tube bundle (CTB) and the ACF tube bundle (ACFTB). The air tunnel was an open-type win tunnel that generated airflow across the test section. The cross-section of the wind tunnel had a square shape of 300 mm x 300 mm. The tunnel was insulated with a rubber sheet insulation. The air from the surrounding

was sucked by a suction fan and flowed through the wind tunnel. Air velocity can be regulated by tuning an inverter of the suction fan. Three upstream points were imposed to measure airspeed by a hot-wire anemometer. The pressure drop of the test section was measured by a digital manometer.

(ii) Hot water circuit: water was heated by a 2-kW electric heater installed in a water tank. The hot water was pumped through the flow meter and was fed to the test section. The flow meter worked in the range of 0.8-18.0 LPM. This circuit aimed to transfer heat from the hot water to the airflow over the test section.

(iii) Test section: two test sections consisted of CTB and ACFTB which the tube bundles were an inline tube arrangement. It had two tube rows that comprised 20 parallel tubes per row. All tubes were mounted to both inlet and outlet headers. The frontal area was designed as 270 mm x 255 mm. In this study, two working fluids were defined as one fluid mixed (air) and another fluid unmixed (water). The geometrical details of the test tube bundles are displayed in Figure 3. The test section specifications are informed in Table 1.

(iv) Data acquisition system: T-type thermocouples were employed to measure temperature during the test run. Upstream and downstream were measured in five positions of square cross-section as a top, bottom, right, left, and center regions. Also, the water temperatures at the inlet and outlet of the test section were collected. All temperature measurements were recorded by a data logger.

The experimental conditions were set to constant mass flow rate and inlet temperature of the water. At the same time, the airflow was varied to raise the Reynolds number (Re). The test conditions are shown in Table 2. Additionally, the accuracies of the measurements are displayed in Table 3.

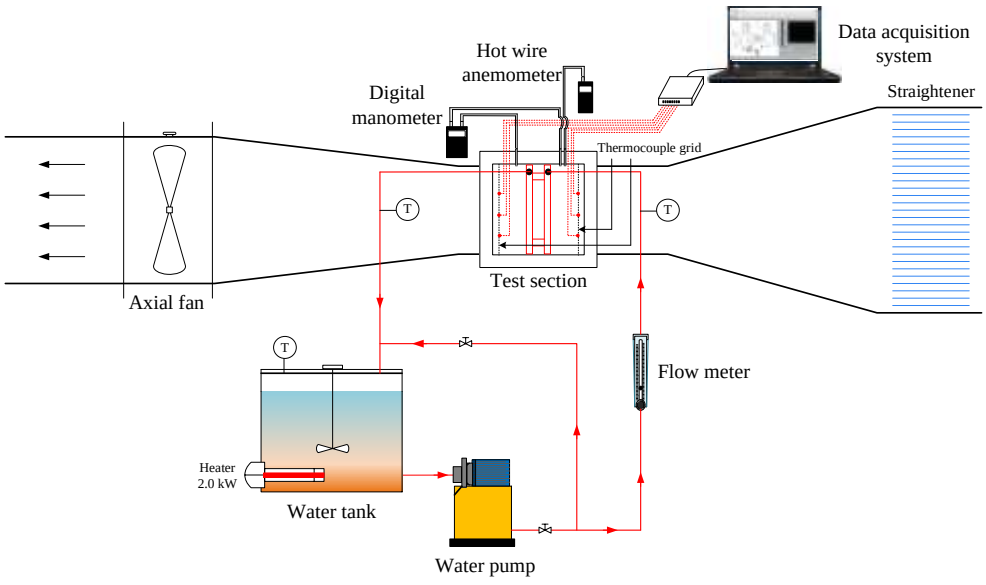

Figure 2 The schematic diagram for the CTB and ACFTB investigation

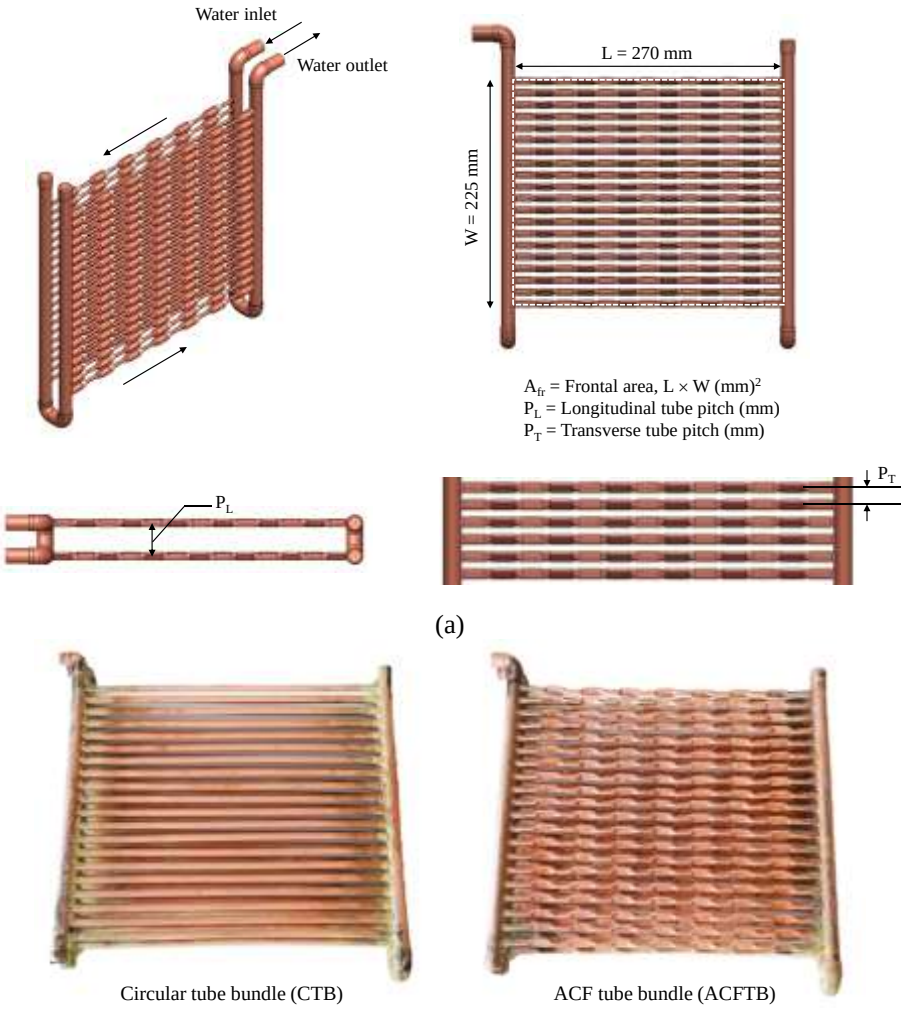

Figure 3 Geometric details of the test tube bundles: (a) dimension details of the test section and (b) photograph of the test sections

Table 1 Specification of the test sections

Parameters	CTB	ACFTB
Tube characteristics	Circular	ACF
Outer diameter of circular tube ($D_{o,cir}$)	6.35 mm	6.35 mm
Outer hydraulic diameter ($D_{h,o}$)	6.35 mm	4.75 mm
Tube pitch (P)	-	20 mm
Longitudinal tube pitch (P_L)	16.35 mm	16.35 mm
Transverse tube pitch (P_T)	11.35 mm	11.35 mm
Frontal area (A_{fr})	0.06 m^2	0.06 m^2
Minimum free flow area (A_{min})	0.026 m^2	0.026 m^2
Total surface area (A_o)	0.215 m^2	0.217 m^2

Table 2 Test conditions

Parameters	Conditions
Inlet air dry bulb temperature	30-40 °C
Inlet water temperature	50-60 °C
Frontal air velocity	1-5 m/s
Water mass flow rate	0.13 kg/s

Table 3 The accuracies of the measurement

Equipment	Accuracy
Variable-flow meter of water	±0.5% of full scale
T-Type thermocouple	±0.5°C
Hot wire anemometer	±(0.03 m/s + 5% of mv)
Digital manometer	±1.5% of full scale

3.3 Data reduction

The effectiveness-NTU (ε-NTU) was applied to evaluate the thermal performance of the heat exchanger. The following procedures are adopted to examine the UA value from the collected data in the individual test run.

The rate of heat transfer at the air-side is calculated by

$$\dot{Q}_a = \dot{m}_a C_{p,a} \left(T_{a,out} - T_{a,in}\right) \quad (1)$$

where $\dot{Q}_a$ is the rate of heat transfer of air, $\dot{m}_a$ is the mass flow rate of air, $C_{p,a}$ is the specific heat of air, and $T_{a,out}$ and $T_{a,in}$ are the temperature of the air at the outlet and inlet, respectively.

The rate of heat transfer at the water-side is defined as

$$\dot{Q}_w = \dot{m}_w C_{p,w} \left(T_{w,in} - T_{w,out}\right) \quad (2)$$

where $\dot{Q}_w$ is the heat transfer rate of water, $\dot{m}_w$ is the mass flow rate of water, $C_{p,w}$ is the specific heat of water, and $T_{w,out}$ and $T_{w,in}$ are the temperature of water at the outlet and inlet, respectively.

The total rate of heat transfer ($\dot{Q}_{avg}$) is averaged from the air-side and water-side as follows.

$$\dot{Q}_{avg} = \frac{\dot{Q}_a + \dot{Q}_w}{2} \quad (3)$$

The counter-crossflow heat exchanger that one fluid mixed and another one unmixed is investigated. The U can be solved by using the correlations of the ε-NTU. For N_{row} = 2, the correlations of the multipass counter-crossflow are given as

For C_{min} is fluid A: $$\varepsilon_A = 1-\left(\frac{K}{2}+\left(1-\frac{K}{2}\right)e^{2K/C_A^*}\right)^{-1},\ K = 1-e^{-NTU_A \cdot C_A^*/2} \quad (4)$$

and C_{min} is fluid B: $$\varepsilon_B = \frac{1}{C_B^*}\left[1-\left(\frac{K}{2}+\left(1-\frac{K}{2}\right)e^{2KC_B^*}\right)^{-1}\right],\ K = 1-e^{-NTU_B/2} \quad (5)$$

where $C^* = \frac{C_{min}}{C_{max}}$; C_{min} and C_{max} are equal to C_h / C_c or C_c / C_h that depends on the heat capacity rates of hot and cold fluids. Fluid A is mixed, and fluid B is unmixed.

The effectiveness of heat transfer (ε) is given as

$$\varepsilon = \frac{\dot{Q}_{avg}}{\dot{Q}_{max}} \quad (6)$$

The maximum rate of heat transfer ($\dot{Q}_{max}$) depends on the minimum heat capacity rate (C_{min}) and the maximum temperature variation of each fluid (ΔT_{miax}). The $\dot{Q}_{max}$ can be determined as

$$\dot{Q}_{max} = \left(\dot{m}C_p\right)_c \left(T_{h,in} - T_{c,in}\right), \text{ if } C_c < C_h \quad (7)$$

or

$$\dot{Q}_{max} = \left(\dot{m}C_p\right)_h \left(T_{h,in} - T_{c,in}\right), \text{ if } C_h < C_c \quad (8)$$

The U can be calculated by applying the NTU equation. That is,

$$NTU = \frac{UA}{C_{min}} \quad (9)$$

The j-Colburn factor is a representative in order to assess the air-side thermal performance, as follows

$$j = \frac{h_o}{\rho_a v_{max} C_p} Pr^{2/3} \quad (10)$$

where ρ_a is the density of air, $v_{\max}$ is the maximum velocity of air, and C_p is the specific heat capacity of air.

Fanning friction factor (f) is assigned to assess the flow resistance. The well-known correlation was proposed by Kays and London (1984) that presented in the form of the f-friction factor, as follows.

$$f = \left(\frac{A_{min}}{A_o}\right)\left(\frac{\rho_m}{\rho_{a,in}}\right)\left[\frac{2\Delta P \rho_{a,in}}{G_c^2} - \left(1+\sigma^2\right)\left(\frac{\rho_{a,in}}{\rho_{a,out}} - 1\right)\right] \quad (11)$$

where A_{min} is the minimum free flow area, A_o is the total heat transfer surface area, σ is the ratio of minimum free flow area to frontal area (A_{min}/A_{fr}), G_c is the air mass flux at the minimum flow area, and ρ_m is the average density between $\rho_{a,in}$ and $\rho_{a,out}$.

4. Results and Discussion

Before measuring air-side thermal performance, the deviation of heat transfer rate between hot and cold fluids was validated for all test tube bundles, as illustrated in Figure 4. The result revealed that the deviations of Q_w and Q_a were in the range of error ±10%.

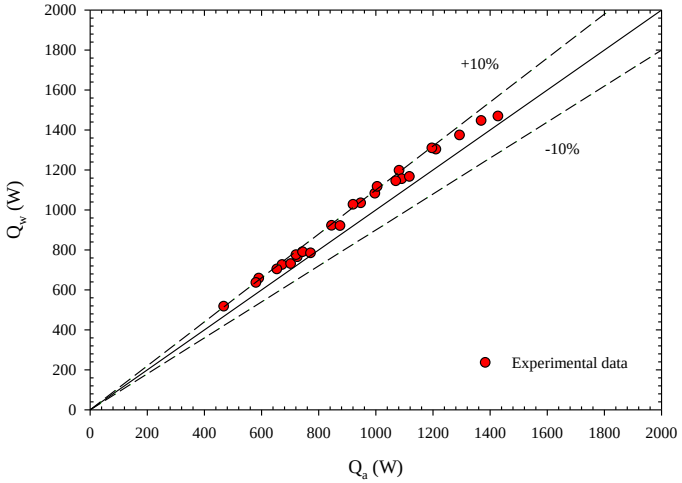

Figure 4 The deviation between Q_w and Q_a

4.1 Heat transfer and pressure drop characteristics

Heat transfer and pressure drop characteristics results of the different tube geometry are explained in this section. For CTB, the variations of the heat transfer rate and the heat transfer coefficient were plotted as a function of the frontal velocity, as respectively illustrated in Figure 5a and Figure 5b. Those plotted were under the water mass flow rate of 0.13 kg/s, and different inlet water temperatures of 50, 55, and 60 °C. The results revealed that the heat transfer rate and heat transfer coefficient gradually increased with increasing frontal velocity. It can be explained as the higher air velocity induced a good mixing, resulting in a better thermal performance. In addition, an increase in inlet water temperature led to enhancing the heat transfer rate (see Figure 5a). That is due to the higher temperature difference between hot and cold fluids. Figure 5b displays the plot of the heat transfer coefficient against the frontal velocity. This figure presented the heat transfer coefficient almost coincided when the inlet water temperatures of 50, 55, and 60 °C. It may come from slightly different values of water thermophysical properties under these test conditions.

Likewise, the heat transfer rate and the heat transfer coefficient of the ACFTB were demonstrated in Figure 6a and Figure 6b, respectively. The experimental results of the heat transfer rate, the heat transfer coefficient, and the effect of inlet water temperature on thermal performance were reported as the same tendency as the results from the CTB.

Figure 7 depicts the variation of the pressure drop as a function of frontal velocity for the different inlet water temperatures. It was observed that the overall trend was increased with increasing the frontal velocity. However, it seemed a negligible effect at all inlet water temperatures. Both CTB and ACFTB reported the same pressure drop tendency, as respectively presented in Figure 7a and Figure 7b.

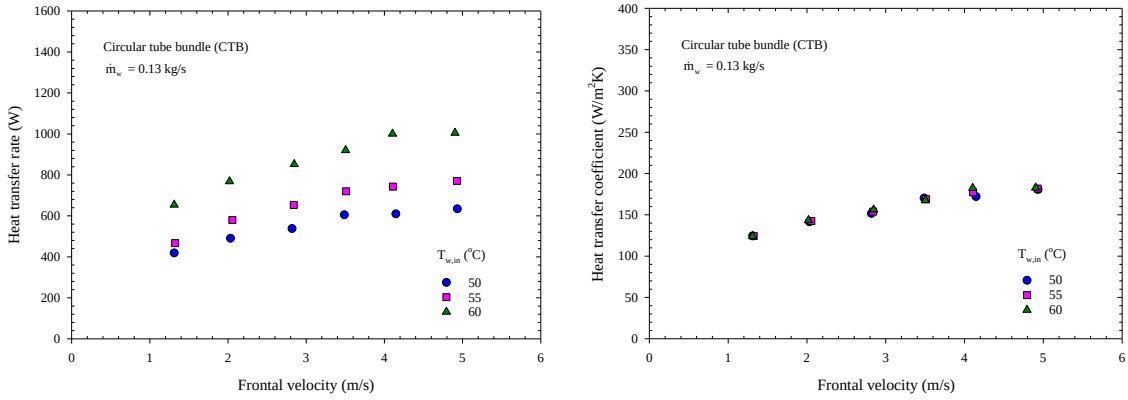

(a) (b)

Figure 5 Air-side performance of the CTB: (a) heat transfer rate, and (b) heat transfer coefficient

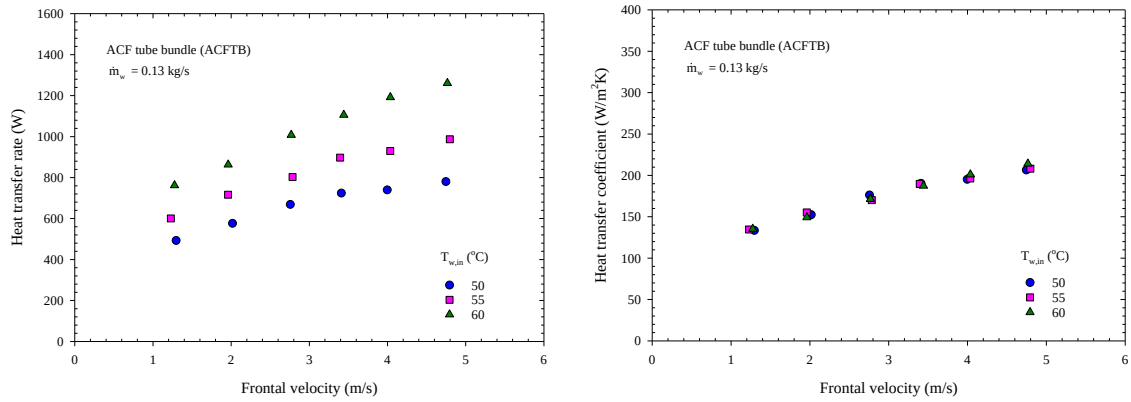

(a) (b)

Figure 6 Air-side performance of the ACFTB: (a) heat transfer rate, and (b) heat transfer coefficient

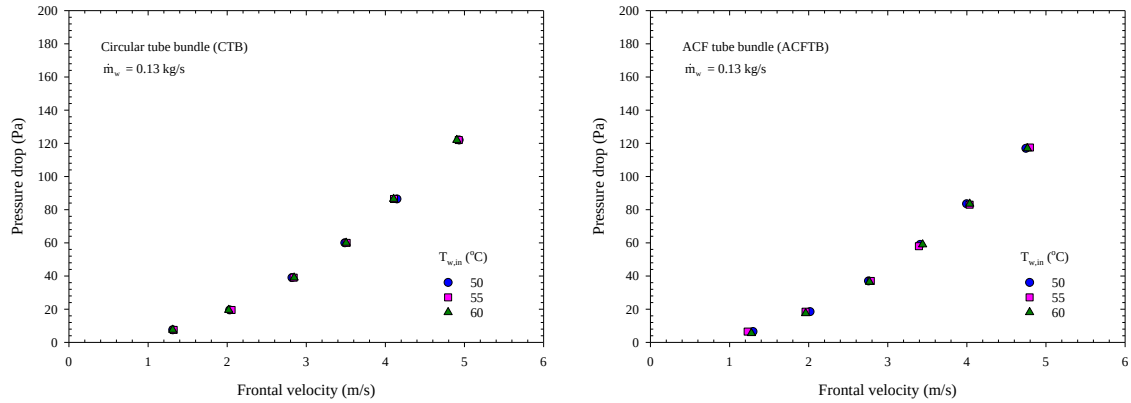

(a) (b)

Figure 7 Pressure drop across test tube bundles: (a) CTB, and (b) ACFTB

4.2 Analysis of thermal-hydraulic performance

The j-Colburn factor and f-friction factor were plotted against the Re at a constant water mass flow rate of 0.13 kg/s and inlet water temperature of 60 °C. Those plots are often applied to analyze the heat exchanger performance, as revealed in Figure 8a (j-Colburn factor) and Figure 8b (f-friction factor).

Figure 8a interprets that the j-Colburn factor gradually decreased with increasing the Re. However, the j-Colburn factor of the ACFTB was better than that of the CTB by approximately 16.3-19.7%. It can be explained that the ACF tube induced a good mixing in the airflow, resulting in the outstanding heat transfer enhancement in the ACFTB. Figure 8b indicated that the f-friction factor gradually increased with increasing the Re from 1,700 to 5,500; however, the f-friction factor was almost unchanged when the Re was greater than 5,500. In comparison, the f-friction factor of the ACFTB was lower than that of CTB, about 1.6-23.8%.

For the performance evaluation criteria, the goodness factor (j/f) was introduced to assess the heat exchanger performance. It was a direct comparison between the j-Colburn factor and the f-friction factor. The goodness factor employs to determine which heat exchanger has the smallest frontal area required for the same pressure drop. j and f values are dimensionless quantities; therefore, they are independent of the hydraulic diameter (D_h). Moreover, when the goodness factor is compared for different surfaces: it reveals the influence of the cross-sectional shape regardless of the geometry scale. The variation of the goodness factor was plotted against the Re, as displayed in Figure 8c. The plot showed that the goodness factor decreased with increasing the Re. By comparison, the goodness factors indicated that the ACFTB showed better performance, about 12.6-46.3%, compared with the CTB.

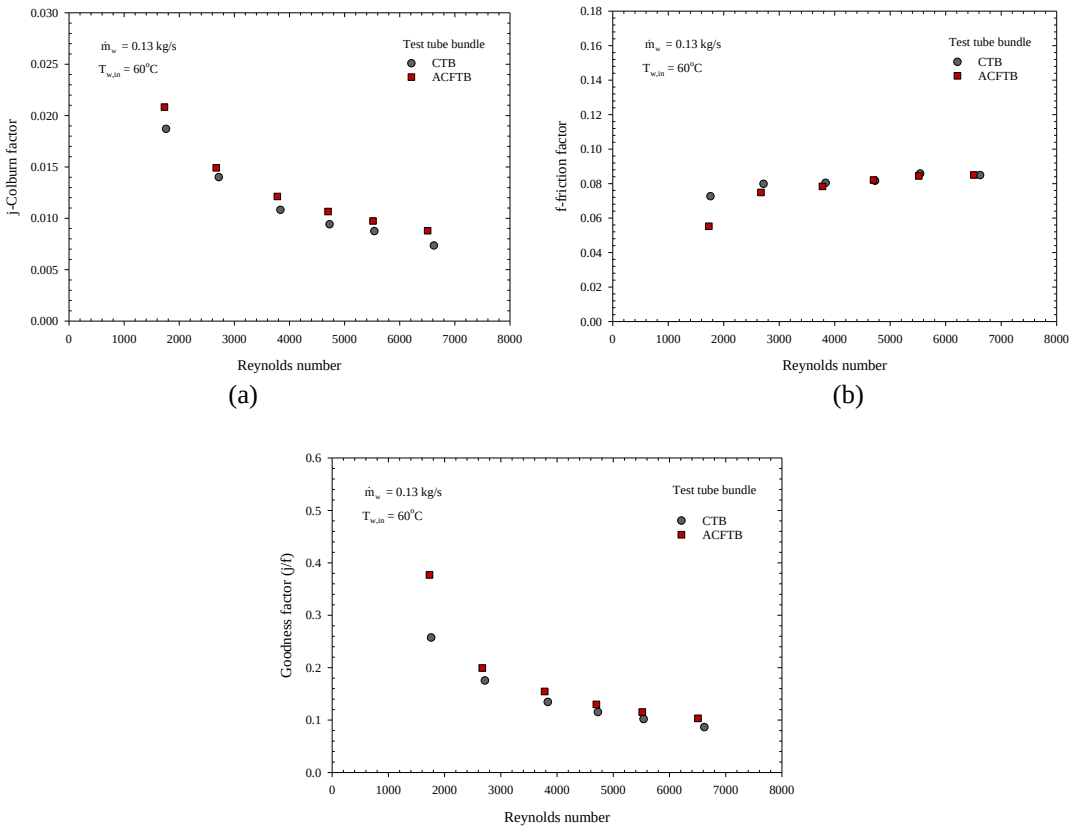

Figure 8 Effect of tube geometry on the (a) j-Colburn factor, (b) f-friction factor, and (c) goodness factor for CTB and ACFTB

4.3 Comparison of thermal-hydraulic performance

The heat transfer coefficient, pressure drop, and goodness factor ratios were utilized to assess the tube bundle performance at a constant water mass flow rate of 0.13 kg/s and inlet water temperature of 60 °C, as presented in Figure 9. Those ratios were defined as the value of an ACFTB divided by a CTB. Figure 9a depicts the comparison of the ACFTB and CTB in terms of heat transfer coefficient ratio. The result showed that the heat transfer enhancement ratio of the ACFTB was higher than that of the CTB by approximately 1.08-1.17 times. On the other hand, the pressure drop ratio of the ACFTB was 0.73-0.98 times lower than that of the CTB, as illustrated in Figure 9b. Moreover, the goodness factor ratio of the ACFTB was greater than 1. Therefore, it meant that the performance of the ACFTB was better than the CTB by approximately 1.13-1.46 times, as exhibited in Figure 9c.

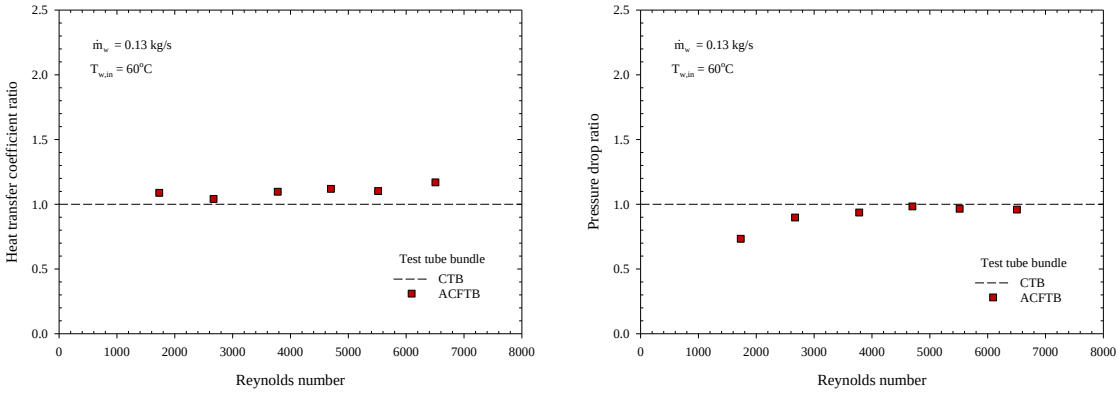

Figure 9 Comparison of air-side performance on the (a) heat transfer coefficient ratio, (b) pressure drop ratio, and (c) goodness factor ratio for CTB and ACFTB

5. Conclusion

This work carried out the thermal-hydraulic performance of the CTB and ACFTB placed in a crossflow. Both test tube bundles were inline tube arrangements with two tube rows. Each row comprised a segment length (L) of 270 mm and segment width (W) of 225 mm. The significant findings can be concluded as below.

1. The heat transfer rate, heat transfer coefficient, and pressure drop tended to increase with the frontal velocity. An increase in the inlet water temperature led to the heat transfer rate increase. However, an increase in the temperatures was a negligible difference in the heat transfer coefficient and pressure drop.
2. In analysis, the j-Colburn factor of the ACFTB was greater than that of the CTB by approximately 16.8-19.7%. On the contrary, the f-friction factor of the ACFTB was lower than that of the CTB by approximately 1.6-23.8%.
3. In comparison, the ACFTB was a better performance than the CTB by (i) higher heat transfer coefficient of 1.08-1.17 times, (ii) lower pressure drop of 0.73-0.98 times, and (iii) higher goodness factor of 1.13-1.46 times.

6. Acknowledgements

The authors are deeply grateful to the National Research Council of Thailand (NRCT), Saijo Denki International Co., Ltd., and Research and Researcher for Industries (RRI) PhD. Program [Grant no. PHD62I0029] for providing financial support to this work.

7. References

Alawadhi, E. M. (2010). Laminar Forced Convection Flow Past an In-Line Elliptical Cylinder Array With Inclination. *Journal of Heat Transfer*, *132*(7), 071701 (10).

Chatterjee, D., & Mondal, B. (2013). Unsteady mixed convection heat transfer from tandem square cylinders in cross flow at low Reynolds numbers. *Heat and Mass Transfer*, *49*(7), 907–920.

Chen, W.-L. (2007). A numerical study on the heat-transfer characteristics of an array of alternating horizontal or vertical oval cross-section pipes placed in a cross stream. *International Journal of Refrigeration*, *30*(3), 454–463.

Guo, Z. Y., Li, D. Y., & Wang, B. X. (1998). A novel concept for convective heat transfer enhancement. *International Journal of Heat and Mass Transfer*, *41*(14), 2221–2225.

Kays, W. M., & London, A. L. (1984). *Compact heat exchangers*. McGraw-Hill.

Li, X., Zhu, D., Yin, Y., Liu, S., & Mo, X. (2018). Experimental study on heat transfer and pressure drop of twisted oval tube bundle in cross flow. *Experimental Thermal and Fluid Science*, *99*, 251–258.

Mangrulkar, C. K., Dhoble, A. S., Deshmukh, A. R., & Mandavgane, S. A. (2017). Numerical investigation of heat transfer and friction factor characteristics from in-line cam shaped tube bank in crossflow. *Applied Thermal Engineering*, *110*, 521–538.

Mangrulkar, C. K., Dhoble, A. S., Chamoli, S., Gupta, A., & Gawande, V. B. (2019). Recent advancement in heat transfer and fluid flow characteristics in cross flow heat exchangers. *Renewable and Sustainable Energy Reviews*, *113*, 109220.

Mirabdolah Lavasani, A., Bayat, H., & Maarefdoost, T. (2014). Experimental study of convective heat transfer from in-line cam shaped tube bank in crossflow. *Applied Thermal Engineering*, *65*(1), 85–93.

Roshko, A. (1955). On the Wake and Drag of Bluff Bodies. *Journal of the Aeronautical Sciences*, *22*(2), 124–132.

Rukruang, A., Chimres, N., Kaew-On, J., Mesgarpour, M., Mahian, O., & Wongwises, S. (2022). A critical review on the thermal performance of alternating cross-section tubes. *Alexandria Engineering Journal*, *61*(9), 7315–7337.

Sayed Ahmed, S. E., Ibrahiem, E. Z., Mesalhy, O. M., & Abdelatief, M. A. (2015). Effect of attack and cone angels on air flow characteristics for staggered wing shaped tubes bundle. *Heat and Mass Transfer*, *51*(7), 1001–1016.